1997-09-01

Microtexture and grain boundary evolution during microstructural refinement processes in SUPRAL 2004

McNelley, T.R.; McMahon, M.E.

Springer

Journal Name: Metallurgical and Materials Transactions. A, Physical Metallurgy and Materials Science; Journal Volume: 28; Journal Issue: 9; Other Information: PBD: Sep 1997
https://hdl.handle.net/10945/60983

Microtexture and Grain Boundary Evolution during Microstructural Refinement Processes in SUPRAL 2004

TERRY R. McNELLEY and MICHAEL E. McMAHON

Electron backscatter pattern (EBSP) analysis of as-processed, processed and annealed, and superplastically deformed specimens of commercially processed SUPRAL 2004 material has been employed to reveal the boundary misorientation distribution and evolution. Earlier studies using X-ray diffraction (XRD) and transmission electron microscopy on this alloy have attributed the transition to microstructures capable of supporting extensive superplastic flow to continuous recrystallization occurring early in the deformation process. The micro- and mesotextural data of the present study show that the deformation texture evident in the as-processed material persists without the formation of recrystallization texture components and remains up to the apparent onset of the grain boundary sliding (GBS) regime. Comparison of the correlated and uncorrelated boundary misorientation data illustrates that the development of boundaries misoriented by ~5 to 15 deg is not random in nature. There is no evidence of recrystallization involving the formation and migration of high-angle boundaries during the refinement process. Microtextural and boundary data from this study provide evidence that the microstructural transition enabling superplastic mechanical behavior of SUPRAL 2004 may be described by a recovery-dominated, continuous process involving the development of moderately misoriented boundaries and leading to a refined microstructure with a boundary distribution of low interfacial energy character.

I. INTRODUCTION

THE engineering development of aluminum alloys thermomechanically processed to achieve extensive fine-grained superplasticity has generally followed one of two basic processing schemes. The first developed was the SUPRAL process, reported by Grimes[1] and Watts *et al.*[2] to involve dynamic recrystallization. The alloy, nominally Al − 6.0 wt pct Cu − 0.4 wt pct Zr, evolves to a microstructure capable of superplastic flow at commercial forming strain rates, $\dot{\varepsilon} > \sim 10^{-2}\ s^{-1}$, only upon deformation and with a microstructural transition occurring early in the deformation process. The Rockwell process, developed later by Paton and Hamilton[3] and initially used for processing of aluminum alloy AA7475, has been reported[4] to involve the development of coarse particles through aging or thermomechanical processing (TMP) to assist in a discontinuous recrystallization during TMP or post-TMP annealing in a manner which may be described by the particle-stimulated nucleation theory of Humphreys.[5]

The latter process is thought to involve conventional recrystallization mechanisms, as defined by Doherty *et al.*[6] to include the formation and migration of high-angle boundaries. The microstructural transition in the SUPRAL process has not been as well described. A comprehensive study was conducted by Bricknell and Edington using X-ray diffraction (XRD) and the crystallite orientation distribution function to quantify textural changes associated with the microstructural evolution in this material.[7] Their study hypothesized that *continuous* recrystallization mechanisms involving the movement of dislocations and dislocation networks were associated with the microstructural evolution to a superplastic microstructure in the alloy. They followed this study with a similar one using transmission electron microscopy to examine the as-processed alloy and found evidence of a banded structure with a large number of low-angle boundaries (LABs, $\theta < 5$ deg) and moderately misoriented boundaries (MMBs, 5 deg $\leq \theta <$ 15 deg) to be associated with the process of microstructural refinement. Conclusive evidence regarding the involvement of the LABs and MMBs was lacking due to an absence of data on boundary evolution.

The goal of the present study is to use an interactive electron backscatter pattern (EBSP) method to examine the microtextural changes and boundary evolution in SUPRAL 2004 from the as-processed state, during static annealing, and with increasing strain levels up to the onset of grain boundary sliding (GBS). Discrete boundary character data obtained from the accompanying orientation information may provide more conclusive measurements of the refinement process operative in this alloy. As this material has been reported to be dynamically recrystallizing, application of the EBSP method to investigate small regions of increasing strain in deformed material would be expected to show the evolution of boundary structure from the as-processed material to a microstructure capable of the high superplastic elongations documented for this material. Ultimately, it may be of interest to modify TMP schemes used to process other aluminum alloys to obtain microstructure more closely related to that which results from the SUPRAL process, which apparently yields superior superplastic performance. In order to attempt such an endeavor, a more fundamental understanding of the microstructural refinement during this process is needed.

TERRY R. McNELLEY, Professor and Chairman, is with the Department of Mechanical Engineering, Naval Postgraduate School, Monterey, CA 93943-5146. MICHAEL E. McMAHON, CDR, U.S. Navy, formerly Doctoral Student, Department of Mechanical Engineering, Naval Postgraduate School, is with the Department of the Navy, Naval Sea Systems Command, Arlington, VA 22242-5160.

Manuscript submitted December 27, 1996.

Table I. Alloy Composition (Weight Percent) for the As-Received SUPRAL 2004

	Cu	Zr	Fe	Si	Zn	Mn	Mg	Ti	Li	Al
Cast Number 2004F013	5.66	0.37	0.14	0.06	0.029	0.013	0.003	0.005	0.0001	bal

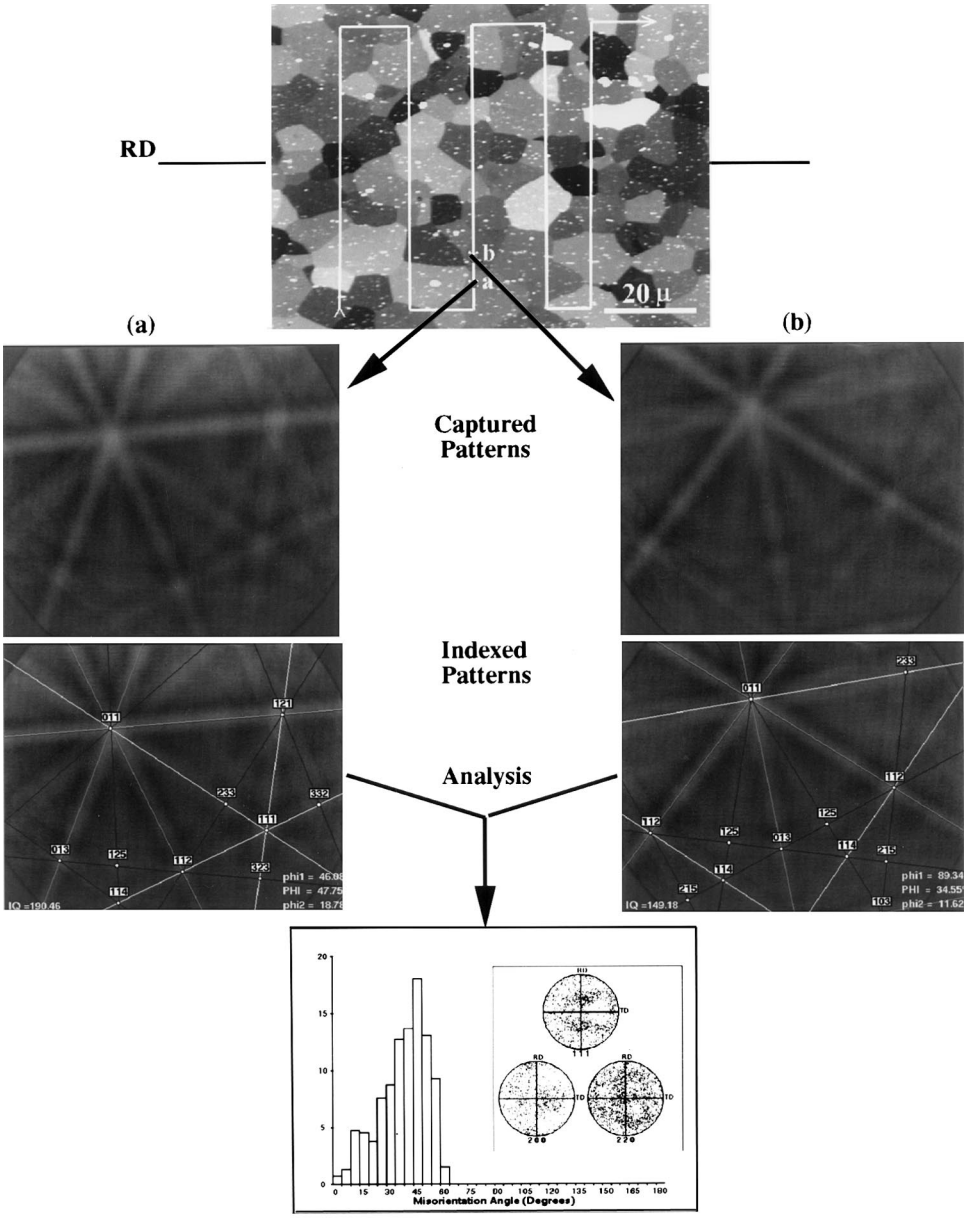

Fig. 1—(*a*) and (*b*) Illustration of the interactive EBSP method employed in this study. Two sequentially captured patterns are collected and indexed. Subsequent analysis of the neighbor orientations produces the boundary information. Data illustrated here were collected from a commercial, superplastic 5083 aluminum alloy that was statically recrystallized during the thermomechanical processing.

II. EXPERIMENTAL PROCEDURE

SUPRAL 2004 material was obtained as 2.0-mm sheet in the as-processed condition from Superform-USA, Inc. (Riverside, CA). The chemical composition is shown in Table I. Tensile coupons were machined with the rolling direction aligned parallel to the tensile direction and deformed in uniaxial tension at a deformation temperature of 450 °C and a constant crosshead speed corresponding to a nominal strain rate of 1.0×10^{-2} s^{-1}. Tensile specimens were deformed to failure and quenched. All deformed tensile coupons were sectioned longitudinally in the tensile direction. Untested coupons (as-processed) and material statically annealed at 450 °C were also sectioned for examination. Electron backscatter diffraction (EBSD) examinations were conducted near the midplane ($t/2$) in the grip (undeformed) region of the tested coupons and at four regions down into the deformed gage section corresponding to increasing levels of strain. Corresponding locations were examined in as-processed and statically annealed materials.

Fundamentals of EBSD techniques have been summarized by Randle.[8] Figure 1 illustrates a typical path of data collection superimposed on a backscattered electron (BSE) micrograph of a representative microstructure. A detailed description of the interactive EBSP analysis method em-

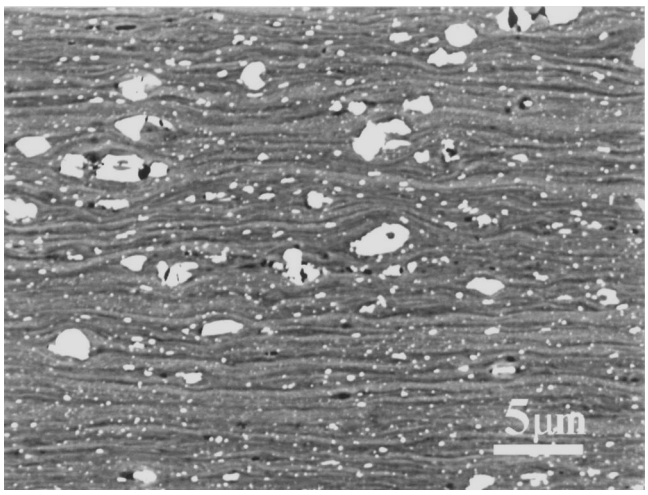

Fig. 2—A BSE micrograph of the as-processed SUPRAL 2004 alloy, illustrating a highly directional microstructure as well as the presence of coarse θ phase (Al_2Cu). The rolling direction is horizontal in the plane of the micrograph. As polished, not etched.

ployed here for collection of orientation information has been given previously.[9,10] In this method, the user positions the electron beam from the scanning electron microscope (SEM) in the spot mode and obtains a diffraction pattern. The pattern is captured and autoindexed by the system software (TexSEM Laboratories, Inc., Provo, UT) to obtain the three Euler angles specifying the lattice orientation relative to the deformation axes associated with processing. Specimen alignment in the EBSD holder in the SEM is arranged to satisfy the default axes assumed in the software. The indexed solution can be visually checked for proper positioning of poles and Kikuchi lines in the diffraction pattern and manually improved if necessary. The electron beam spot is then moved, pixel by pixel, until a change in the pattern is observed. The new pattern is collected, indexed, and stored as denoted by (a) and (b) in Figure 1. Subsequent patterns are obtained as the spot is moved. The path chosen in collecting orientation data was primarily along lines parallel to the through-thickness direction of the specimen, which is also a line of constant working distance in

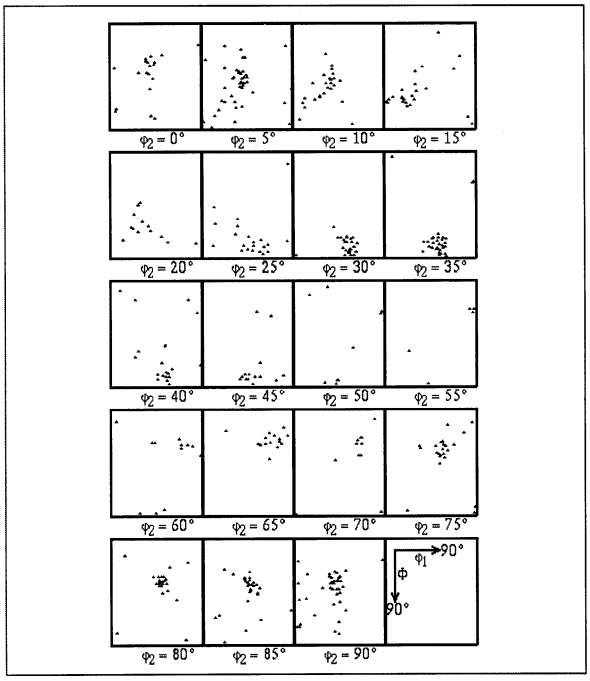

(a)

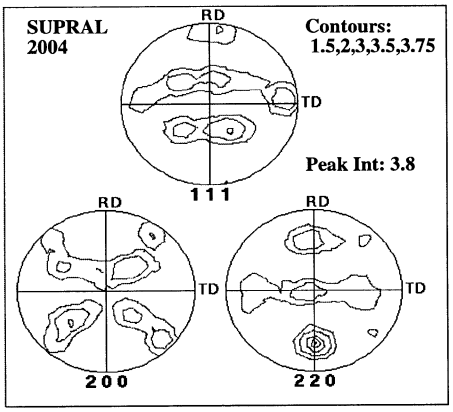

(b)

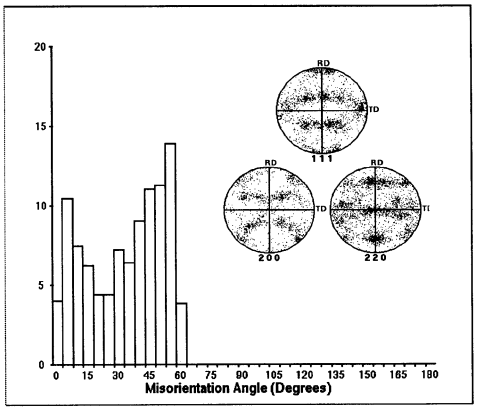

(c)

Fig. 3—Analysis of the orientation data collected from the as-processed specimen of SUPRAL 2004: (*a*) a discrete Euler plot, (*b*) contour pole figure based on the discrete data, and (*c*) misorientation angle histogram with discrete pole figure inserted. A total of 497 orientations were collected sequentially.

Table II. Summary of Boundary Character Data for SUPRAL 2004 Specimens Examined*

SUPRAL 2004	As-Received	30-Minute Static Anneal at 450 °C	6-Hour Static Anneal at 450 °C	12-Hour Static Anneal at 450 °C	Deformed to 16 Pct Strain at 450 °C and 10^{-2} s^{-1}	Deformed to 70 Pct Strain at 450 °C and 10^{-2} s^{-1}	Deformed to 100 Pct Strain at 450 °C and 10^{-2} s^{-1}	Deformed to 132 Pct Strain at 450 °C and 10^{-2} s^{-1}
Total number of Boundaries	496	316	325	326	316	307	303	310
Pct with $\theta < 15$ deg	23.5	26.3	28.9	29.1	20.0	30.6	25.4	15.2
Pct with $\theta > 15$ deg and CSL ($\Sigma < 31$)	9.3	9.2	12.0	12.9	11.0	9.8	10.2	9.4
Pct with $\theta > 15$ deg and disordered	67.3	64.5	59.1	58.0	69.0	59.6	64.4	75.4
Pct $\Sigma 3$ [1.53]	3.0	2.3	3.5	4.7	2.9	4.1	5.0	2.0
Pct $\Sigma 5$ [1.07]	0.6	1.0	.6	0.3	0	0	0	0.3
Pct $\Sigma 7$ [0.86]	0.6	1.3	.6	0.3	3	1.0	1.1	0.7
Pct $\Sigma 9$ [0.88]	1.4	2.3	1.3	0	0	0.3	0.4	0.3
Pct $\Sigma 11$ [0.68]	0.4	0.3	1.3	4.0	1.3	0	0.4	0.7
Pct $\Sigma 13$ a/b [0.59]	0.2	0.3	.3	0.6	1.3	0.3	0.4	1.0
Pct $\Sigma 15$ [0.82]	0.2	0	.3	0.3	1.3	0	0	0.3
Pct $\Sigma 17$ a/b [0.51]	0.6	0.3	.3	1.6	0.6	0.7	1.1	0.7
Pct $\Sigma 19$ a/b [0.48]	0.4	0	.6	0	0.3	0.3	0	1.0
Pct $\Sigma 21$ a/b [0.66]	0.4	0	0	0.6	0.3	0.3	0	1.3
Pct $\Sigma 23$ [0.43]	0	0.3	0	0	0	0	1.1	0
Pct $\Sigma 25$ a/b [0.48]	0.6	1.3	.6	0.6	0.6	1.8	0.4	0.7
Pct $\Sigma 27$ a/b	0.2	0	0	0	1.0	1.0	0.7	0
Pct $\Sigma 29$ a/b	0.8	0	.6	0	0.6	0.3	0.4	0.7

*The numbers in brackets indicate the percent of CSL boundaries expected for random rotations.[19]

the SEM, although a portion of the data was collected during translation of the spot along lines parallel to the tensile axis. Collecting orientation data along a line of constant working distance facilitated pattern indexing in that focusing distortions were minimized. Magnification was maintained between 1000 and 1500 times for all data collection. Analysis of sequentially collected orientation data is accomplished to determine the character of the boundary associated with each successive orientation change (Figure 1). The boundary disorientation, calculated as the minimum rotation angle about an arbitrary axis to bring the *neighboring* crystal orientations into coincidence, is calculated by the system software and displayed in either Euler angle, axis/angle pair, or Rodriguez vector format. The resulting boundary misorientation distribution is *correlated* because the rotation angles calculated in this procedure represent the misorientations of *adjacent* grains.

Microtextural and boundary character analyses were conducted for each of the data sets. In addition, the random distribution of boundary misorientation, with consideration of the influence of the preferred orientation present, was also calculated for each data set and plotted as the *uncorrelated* distribution of misorientation. The random distribution of boundary misorientation considering texture, *i.e.*, the *uncorrelated* misorientation distribution, was calculated by comparing each orientation to all other orientations obtained in the data set. This procedure produced a large set of $(N - 1)^2$ misorientations, where N is the number of orientations. The sorting procedure employed to produce the misorientation distribution considered all $(N - 1)^2$ misorientations, although of these, only $(N(N - 1))/2$ are distinct misorientations.

Finally, BSE micrographs were taken at all regions of the EBSD examination to detail the grain structure, precipitate size, and dispersion. The BSE micrographs were obtained using a TOPCON SM-510 SEM and were obtained at a working voltage of 5 kV to obtain grain orientation contrast as well as atomic number contrast. Standard electropolishing methods described previously were used for both BSE and EBSD examinations.[10]

III. RESULTS

A tensile elongation of 756 pct was obtained for the test conditions used, which compares favorably to the value of 800 pct at essentially the same test conditions and reported by the manufacturer. Figure 2 illustrates the microstructure present in the *as-processed* material. The BSE micrograph of the as-processed material reveals that coarse θ-phase (Al_2Cu) particles are present in addition to a fine dispersion of Al_3Zr particles. Although grain contrast is not evident in the as-processed material, directionality is apparent in the microstructure, presumably due to mechanical fibering introduced in the final cold rolling process. The original grains are thought to be flattened and thinned by the rolling process and elongated in the (apparent) rolling direction.

Figures 3(a) through (c) illustrate the microtexture and mesotexture of the as-processed material. Analysis of the Euler plot, Figure 3(a), indicates that the microtexture in the as-processed material is a deformation texture consistent with aluminum alloys rolled to high strain at low to moderate temperatures and is also consistent with the results of earlier XRD studies.[11] The texture extends along the β-fiber, with the strongest component concentration near the

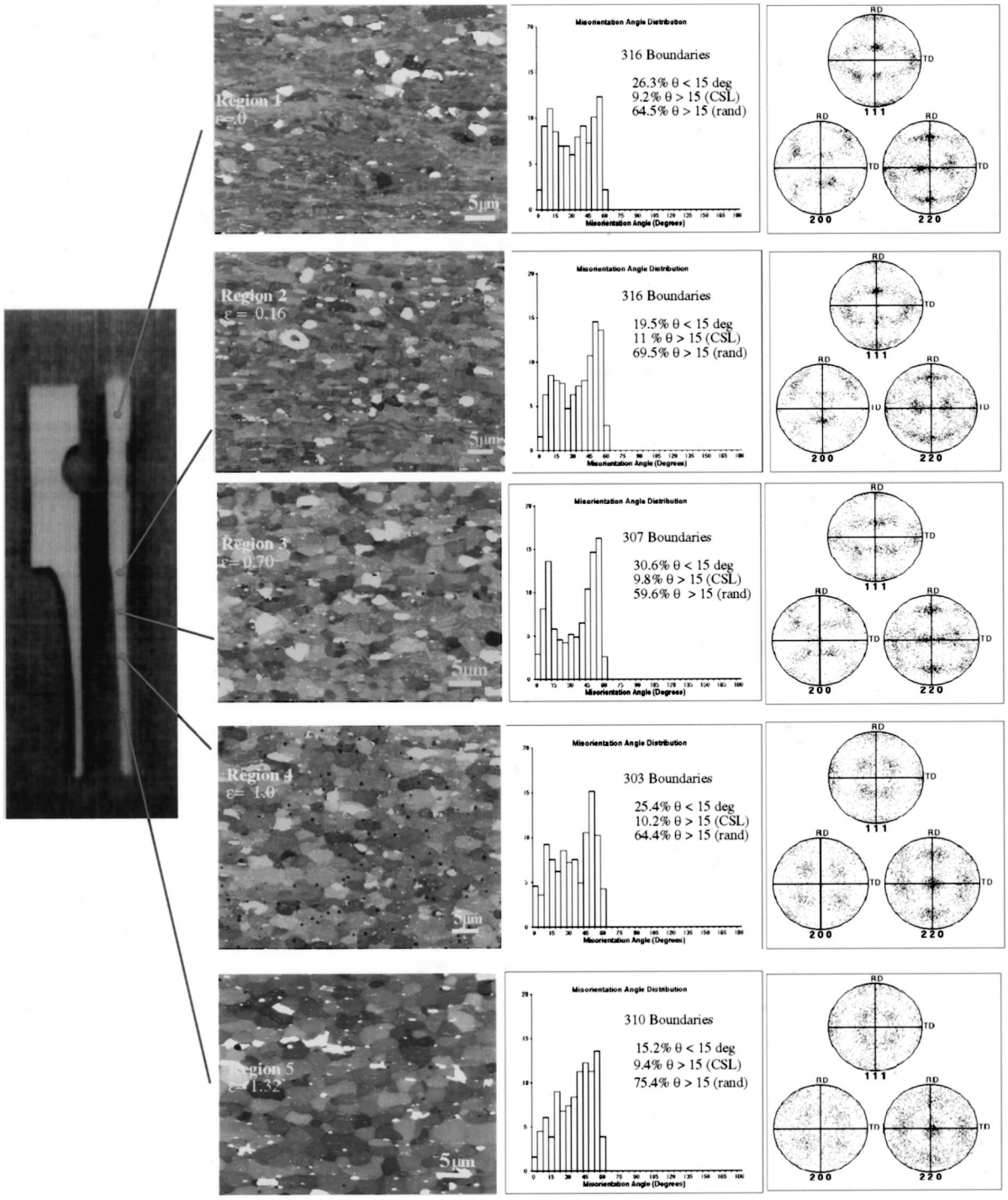

Fig. 4—BSE micrographs, boundary misorientation plots, and discrete pole figures for five selected regions in a SUPRAL 2004 tensile specimen deformed to failure.

S, {123} ⟨634⟩, and brass, {011} ⟨211⟩, orientations. A closely grouped cluster of grains with orientations near S is evident in the $\varphi_2 = 35$ deg window of the Euler plot, while orientations near brass are identified readily in the $\varphi_2 = 90$ deg window. The other significant deformation component is the S/B orientation, {168} ⟨211⟩, identifiable in the $\varphi_2 = 5$ deg and $\varphi_2 = 80$ deg plots. The formation of such a texture has been attributed to stable orientations resulting from multiple slip on limited {111} ⟨110⟩ systems in fcc metals and the influence of twinning on the generation of new orientations.[7,12] Figure 3(b) shows the contour pole figure constructed from the discrete data.

In Figure 3(c), the distribution of boundaries by misorientation angle is graphed. A bimodal appearance of the distribution is evident. The boundary data (quantified later in Table II) indicates that the as-processed material possesses a significant fraction (0.235) of MMBs of 5 to 15 deg misorientation. During data collection, orientations were captured at spacings of ≈0.5 μm, while the thickness of the pancaked grains is ≈2 to 3 μm. Therefore, the misorien-

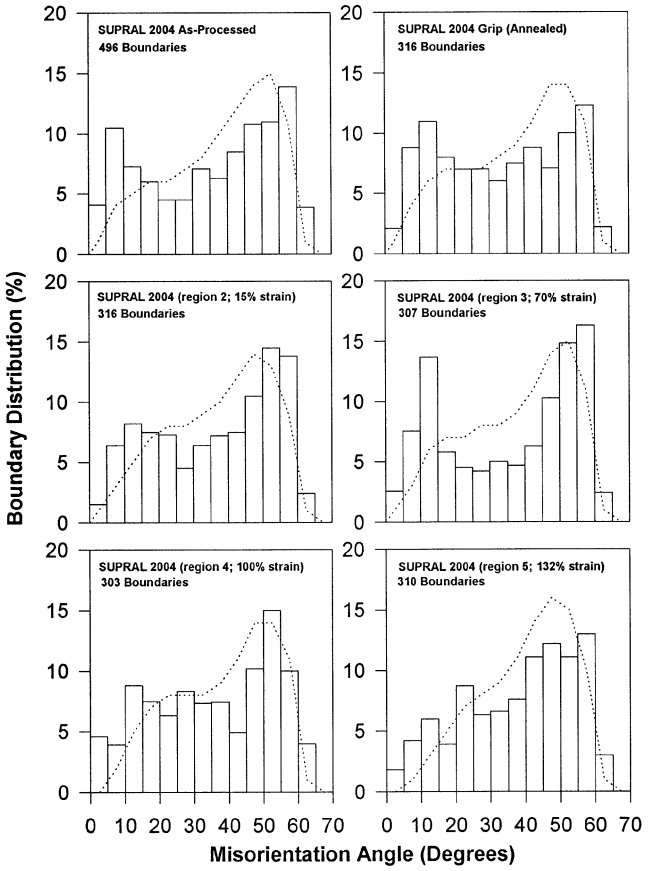

Fig. 5—Misorientation histograms for the as-processed SUPRAL 2004 as well as the regions examined for the deformed tensile sample for this material and represented in Fig. 4. In all cases, the uncorrelated distribution of misorientation is indicated by the dotted line.

tation distribution reflects primarily deformation-induced structure, as well as some prior grain boundaries. Recent studies[13] on pure aluminum have reported that similar deformation-induced structures consist of cells surrounded by dislocation structures with misorientations primarily in the 5 to 15 deg range but including misorientations up to 40 deg. The peak fraction of the high-angle boundaries (HABs, $\theta > 15$ deg) present lies in the 55 to 62.8 deg misorientation range, near that expected if twinning were influential in the generation of new orientations. The quantitative data confirms this observation (and confirms the textural data), as the number of boundaries satisfying the Brandon[14] criterion for nearness to the $\Sigma 3$ CSL is twice the value expected for a random population. Overall, the misorientation distribution is not dominated by disordered HABs with characteristic high interfacial energy values. Rather, the distribution of boundaries present in the as-processed material may be described as reflecting a lower interfacial energy character, with approximately 50 pct of all boundaries either LAB, low-index CSL boundaries, or HABs near the twin relation, 60 deg/$\langle 111 \rangle$.

Figure 4 provides a summary of the BSE micrographs, microtexture, and boundary misorientation data collected from the deformed tensile specimen. These data are isochronal, in that all regions experienced the same time at temperature. The regions examined in the fractured tensile specimen are indicated, accompanied by a BSE image of the region adjacent to the EBSD examination area for the level of local strain approximated by the deformed specimen geometry. A summary of the boundary data, categorized by energy character following Watanabe *et al.*[15] and Haasen,[16] is provided in the corner of each misorientation angle histogram.

Examination of the BSE micrographs in region 1, the undeformed grip section, shows the contrast variation due to LABs and substructure between the bands apparent in Figure 2, also reported in earlier TEM studies[7] in the as-processed material. The material in region 2 has experienced an approximate local strain of 0.16, and some (sub)grain refinement is apparent. A loss in the directionality of the microstructure is also evident. The local strain in region 3 is estimated to be 0.70, and grain refinement processes have resulted in an equiaxed grain structure with a fine, uniform grain size. Some of the diffuse boundaries appear to have sharpened. A mean linear intercept (MLI) calculation indicated an average MLI value of $L_{av} = 5.26$ μm for this structure. In regions 4 and 5, where the local strains are approximately 1.0 and 1.32, respectively, increasing orientation contrast for grains indicates a higher degree of misorientation than in the previous regions of lower strain.

Analysis of the microtexture plots in Figure 4 reveals that the effect of a 30-minute static anneal (the grip section) at the test temperature of 450 °C is a slight sharpening in the texture. The Euler plots (not shown here) indicate a higher fraction of orientations near S (and fewer near brass) as well as the appearance of more orientations near copper, $\{112\}\langle 111\rangle$. The shift away from brass orientations toward copper at elevated temperature has been attributed to the activation of additional slip systems leading to octahedral slip on $\{111\}\langle 110\rangle$ systems.[17,18] The same deformation texture components are observed to persist through straining with noticeable randomization and weakening of texture occurring by an approximate strain of 1.0. Orientations near brass are observed to be preferentially retained. Retention of $\langle 121\rangle$ orientations during grain boundary sliding (GBS) (brass is $\{110\}\langle 112\rangle$) has been previously observed[7] and attributed to concurrent deformation by limited or single slip. As these data were collected isochronally, with all regions experiencing the same time at elevated temperature, the randomizing of texture here may be attributed *only* to GBS. The transition to GBS as the dominant deformation mechanism is then evident as early as a strain of 1.0. There is no evidence of the development of distinct recrystallization texture components during the microstructural refinement processes.

Mesotextural data, depicted here in the boundary misorientation plots, show the retention of a significant fraction, approximately 20 to 30 pct, of MMBs up to the apparent onset of GBS. During the microstructural refinement processes, occurring during early stages of plastic deformation, the misorientation of the MMBs is observed to shift to higher values of misorientation concurrent with retention of the deformation texture. This suggests that recovery mechanisms may be responsible for the development of the MMBs. At the strain level near that which has been associated with completion of the dynamic recrystallization in these alloys, $\varepsilon \approx 0.70$, only 59.6 pct of the boundaries encountered were disordered HABs. Additionally, the fraction of HABs satisfying the Brandon criterion for nearness to exact coincident site lattice (CSL) values is relatively

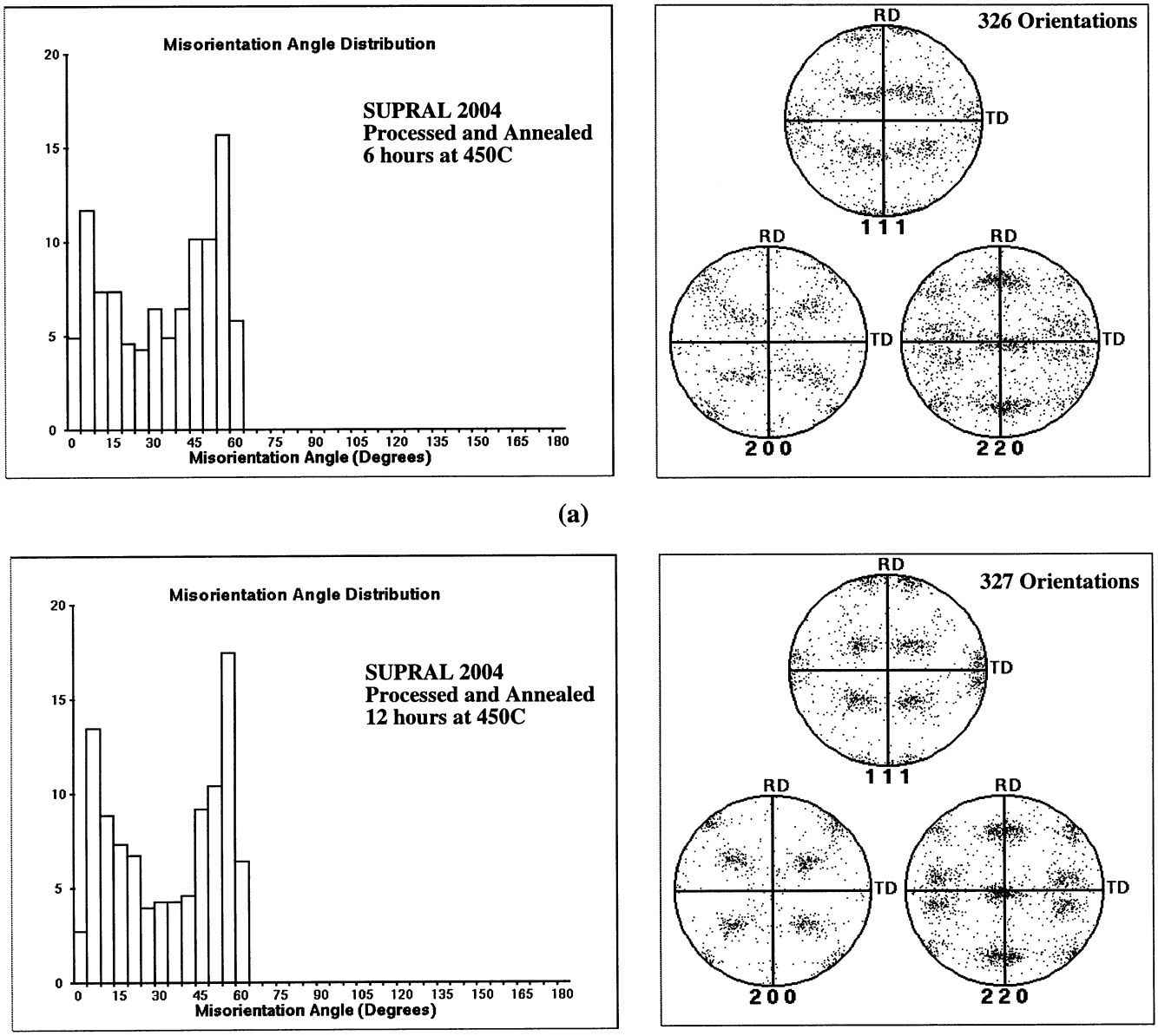

Fig. 6—(*a*) and (*b*) Boundary misorientation distributions and discrete pole figures for the SUPRAL 2004 material during static annealing at 450 °C. The microtextural components remain unchanged, while the overall strength of the texture sharpens. The misorientation plot tends toward a pronounced bimodal distribution with the peak fraction of the HABs near the twin misorientation of 60 deg.

constant and near that expected from purely geometrical considerations.[19]

Figure 5 is a summary of the misorientation graphs with the plot of the uncorrelated (''random'') distribution, expected from the material given the preferred orientation present, superimposed. Through deformation to strains at which the microstructural refinement processes are thought to be complete, $\varepsilon \approx 0.70$, the fraction of boundaries in the MMB regime (5 to 15 deg misorientation) is significantly higher than that predicted for a random distribution, even given the effect of texture in the processed material. Because the methodology used in the EBSD examination is known to preclude some boundaries with misorientations less than approximately 2 deg[9] the deviation is likely more pronounced that the plots depict. Additionally, the average misorientation of the MMBs has shifted to higher values, with the largest fraction in the 10 to 15 deg misorientation range by an approximate strain of 0.70. This suggests that the microstructural refinement process may include the development of MMBs directly from the cell walls of the deformation-induced structures of the as-processed material by recovery processes, but with little buildup of misorientation. At higher strain values, where deformation by GBS is thought to dominate, a reduction of LABs occurs concurrent with a shift in the boundary misorientation distribution toward a random distribution. As the texture diminishes, the uncorrelated misorientation data will approach that described by Mackenzie[20] for randomly oriented cubes.

Figure 6 illustrates the microtexture and boundary evo-

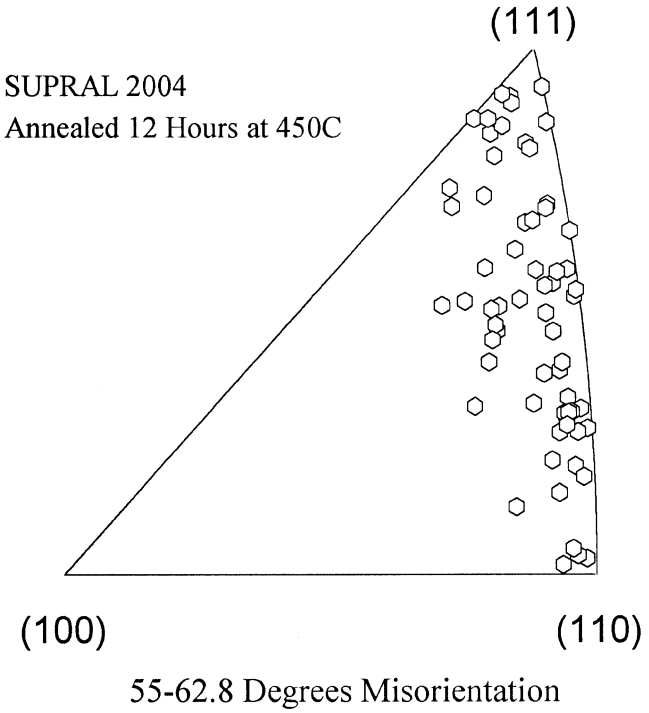

Fig. 7—The grain misorientation texture illustrating the distribution of grain rotation axes for boundaries with misorientations of 55 to 62.8 deg for material statically annealed at 450 °C.

lution during static annealing at 450 °C. The microtexture sharpens during annealing with the same deformation texture components persisting during the annealing. There is no textural evidence of primary recrystallization involving the formation and migration of HABs during prolonged static annealing. The accompanying boundary misorientation data show that the bimodal distribution becomes more pronounced. At the end of the 12-hour anneal, a significant fraction (0.31) of all HABs are within 55 to 62.8 deg misorientation, near the twin orientation ($\Sigma 3$, 60 deg/$\langle 111 \rangle$). Figure 7 shows the grain misorientation texture for boundaries in this region in the specimen statically annealed for 12 hours. Additionally, over 24 pct of all boundaries are MMBs by the end of the 12-hour static anneal. The data suggest that boundary development during static annealing of this alloy may be described by development and refinement of MMBs and, separately, annealing twinning processes. It is noted that the MMB development during static annealing mirrors that observed during deformation. This provides more evidence that the refinement processes in this alloy are continuous from the onset of heating to the deformation temperature and confined to the dynamic regime.

Table II summarizes the quantitative data for boundary character analysis. With the exception of LABs/MMBs ($\Sigma 1$) and twin boundaries ($\Sigma 3$), the CSL data are unremarkable, and the overall fraction of CSL boundaries with $3 \leq \Sigma \leq 25$ does not deviate significantly from the value predicted by purely geometrical considerations ($\approx$9.0 pct for Brandon nearness criteria). The absence of higher order, twin-related CSLs, particularly $\Sigma 27a/b$, would imply that all of the randomization of texture in the more highly strained regions of the isochronally collected data may be attributed to GBS. The presence of $\Sigma 3$ boundaries at levels 2 to 3 times that expected for a random distribution of orientations suggests that twinning may be important in the generation of new orientations during the microstructural refinement processes. This observation is consistent with the predominance of a brass component to the texture. The overall distribution of boundaries by energy character indicates that the fraction of LABs/MMBs is significantly higher than that predicted by geometrical considerations.

IV. DISCUSSION

The data from this investigation show that, at the completion of the microstructural refinement processes, there is no evidence of recrystallization involving the formation and migration of high-angle boundaries. Rather, the data suggest that continuous, recovery-dominated processes occur from the onset of post-TMP heating and result in the formation of a significant fraction ($\sim$0.25) of well-developed, moderately misoriented boundaries and an overall bimodal distribution of boundary misorientation, with low-energy interfacial energy character, in the superplastically enabled material. Given that the fraction of HABs fulfilling nearness criteria to nontwin, low-index CSL ($3 < \Sigma < 31$) relations is, essentially, constant and near the level predicted for random processes, and that the number of disordered HABs remains nearly constant until well into the GBS regime, it may be concluded that the evolution of the MMBs to higher levels of misorientation by recovery processes is responsible for the microstructural refinement and reduction in grain size and may be assumed to be responsible for enabling superplastic behavior.

Based on this observation, earlier work attributing the transition to a superplastically capable microstructure to dynamic recrystallization should be reconsidered and the refinement process viewed as a continuous process that begins during the TMP and with boundary development and continues through static annealing and dynamic straining. The continuous refinement process involves, primarily, the development of MMBs and may be viewed as a recovery-dominated mechanism. Results from the statically annealed specimens support a continuous model, in that the evolution of MMBs toward higher misorientation values is observed in the absence of deformation. The evolution of HABs in the statically annealed material appears to be associated with annealing twinning and not formation of new HABs during primary recrystallization processes.

Following the (apparent) onset of GBS, MMBs coalesce (preferentially those with lower misorientation, according to the data) during grain rotation and accommodation processes and random micro- and mesotextures result. The preferential retention of brass orientations in deformed regions during randomization of texture due to GBS would strengthen earlier suggestions[7] that slip may be an important accommodation mechanism during GBS processes in these alloys.

V. CONCLUSIONS

1. The microstructural refinement responsible for enabling superplastic behavior in SUPRAL 2004 may be attributed to recovery-dominated processes involving the continuous development of the MMBs found in the as-processed material. The resultant superplastically enabled

microstructure has a characteristically lower boundary-interfacial energy distribution.
2. Recrystallization involving the formation and migration of HABs is not responsible for the microstructural refinement processes observed in this alloy.
3. Evidence suggests that GBS is the dominant deformation mechanism by a strain of 1.0, suggesting that the transition to a superplastic microstructure is achieved prior to a strain of 1.0.
4. Accommodation by slip may be important during the GBS process.

ACKNOWLEDGMENTS

The authors express their appreciation to Mr. A.J. Barnes, SUPERFORM U.S.A., Inc., and Dr. David P. Field, TEXSem Laboratories, Inc., for their assistance in this research.

REFERENCES

1. R. Grimes: *Advances and Future Directions in Superplastic Materials*, NATO-AGARD Neuilly Sur Seine, France, 1988, Lecture Series No. 168, pp. 8.1-8.16.
2. B.M. Watts, M.J. Stowell, B.L. Baike, and D.G.E. Owen: *Met. Sci. J.*, 1976, vol. 10 (6), pp. 189-97.
3. N.E. Paton and C.H. Hamilton: U.S. Patent 4,092,181, 1978.
4. J.A. Wert, N.E. Paton, C.H. Hamilton, and M.W. Mahoney: *Metall. Trans. A*, 1981, vol. 12A, pp. 1267-76.
5. F.J. Humphreys: *Acta Metall.*, 1977, vol. 25, pp. 1323-44.
6. R.D. Doherty, G. Gottsttein, J. Hirsch, W.B. Hutchinson, K. Lucke, E. Nes, and P.J. Wilbrandt: *Report of Panel on Recrystallization Textures: Mechanisms and Experiments*, ICTOM 8, J.S. Kallend and G. Gottstein, eds., TMS, Warrendale, PA, 1988.
7. R.H. Bricknell and J.W. Edington: *Acta Metall.*, 1979, vol. 27, pp. 1303-11.
8. V. Randle: *Microtexture Determination and Its Applications*, The Institute of Metals, London, 1992.
9. T.R. McNelley and M.E. McMahon: *J. Met.*, 1996, vol. 48, p. 2.
10. T.R. McNelley and M.E. McMahon: *Metall. Mater. Trans. A*, 1996, vol. 27A, pp. 2252-62.
11. J. Hirsch and K. Lucke: *Acta Metall.*, 1988, vol. 36 (11), pp. 2883-2904.
12. J.S. Kallend and G.J. Davies: *Phil. Mag.*, 1972, vol. 25, p. 471.
13. G.I. Rosen, D. Juul Jensen, D.A. Hughes, and N. Hansen: *Acta Metall.*, 1995, vol. 43 (7), pp. 2563-79.
14. D.G. Brandon: *Acta Metall.*, 1966, vol. 14, pp. 1479-1484.
15. T. Watanabe, H. Fuji, H. Oikawa, and K.J. Arai: *Acta Metall.*, 1989, vol. 37, p. 941.
16. P. Haasen: *Metall. Trans. A*, 1993, vol. 24A, pp. 1001-15.
17. M. Hatherley and W.B. Hutchison: *An Introduction to Texture in Metals*, The Institute of Metallurgists, London, 1979.
18. R.E. Smallman: *Modern Physical Metallurgy*, Butterworth and Co., London, 1985.
19. D.H. Warrington and M. Boon: *Acta Metall.*, 1975, vol. 23, pp. 599-607.
20. J.K. Mackenzie: *Biometrica*, 1958, vol. 45, pp. 229-40.